Diverse C-Terminal Domains of Paralogous Single-Stranded DNA Binding Proteins: Impacts on Biophysical Properties and Biological Functions in *S. coelicolor*

Goran Pipalović[1,‡], Želimira Filić[1,‡], Mirsada Ćehić[1§], Tina Paradžik[1], Ksenija Zahradka[2], Ivo Crnolatac[3*], Dušica Vujaklija[1*]

‡ Shared first authorship

* Corresponding authors:

Ivo Crnolatac (Ivo.Crnolatac@irb.hr)

Dušica Vujaklija (vujaklij@irb.hr)

Affiliations:

[1]Division of Physical Chemistry, Institute Ruđer Bošković, Zagreb, Croatia

[2]Division of Molecular Biology, Institute Ruđer Bošković, Zagreb, Croatia

[3]Division of Organic Chemistry and Biochemistry, Institute Ruđer Bošković, Zagreb, Croatia

§Present address: University of Applied Sciences in Security and Safety, Zagreb, Croatia

Abstract

Single-stranded (ssDNA) binding proteins play a key role in DNA metabolism. Many taxonomically distant bacteria have additional Ssb proteins, which are still largely unexplored. Given the recent findings on the importance of the C-domain of SSB protein from E. coli, we investigated here the role of different C-domains on the function of paralogous Ssb proteins from the multicellular bacterium Streptomyces coelicolor. Our results revealed that C-domain mutations lead to defects during the bacterial developmental phase and accelerate or decelerate growth and sporulation. In addition, we have shown how mutations of C-domains affect the biophysical and biochemical properties of Ssb proteins, which probably impaired their biological functions. Dynamic light scattering (DLS) analyzes showed that only SsbA, which is essential for survival, can form biomolecular condensates, but this was not dependent on the C-tip, as indicated previously. DLS suggested that C-domains of SsbA and SsbB occupy more globular conformation and that, despite Mw differences, both proteins have similar hydrodynamic diameters. The SsbA is more stable to thermal denaturation than SsbB. The thermodynamic profile of the unfolding transition for Ssb proteins showed that truncated C-domain increases, while mutated decreases the molar unfolding enthalpy. Calorimetric titrations revealed that ssDNA binding causes restrictions in the conformational mobility of studied proteins. We also found that the acidic C-tip of SsbA (DEPPF) aids in achieving the best possible conformation for ssDNA binding. Finally, gel-mobility-shift assays showed that the C-domain is crucial for the cooperative binding of SsbA and also suggested that the C-domain may have an important role in regulating the cooperative binding of SsbB.

Keywords: *Streptomyces coelicolor*, Paralogous SsbA and SsbB proteins, IDL C-domain, chromosome segregation, irregular septation, Biomolecular condensates, Cooperativity, Hydrodynamic properties, Isothermal titration calorimetry

Introduction

Single-stranded DNA binding proteins (SSBs) are essential for the maintenance of genomic integrity in all forms of life[1–8]. SSBs bind, with a high affinity, single-stranded DNA (ssDNA) intermediates that are transiently formed during DNA processing. This binding is sequence-unspecific, and it has importance in protecting ssDNA from nucleolytic degradation and stabilizing ssDNA by preventing its reannealing and secondary structure formation[2,9–11]. So far, SSB has been found to interact with 20 proteins (SIPs) involved in DNA metabolism, it mobilizes them to their place of action and modulates their activities[12–19]. SSB from *Escherichia coli* (EcSSB) has been extensively studied for decades and has become a prototype for investigating the structure and interactions of bacterial SSBs[1,4,7,18,20,21]. *Ec*SSB functions as a homotetramer[22–24] and with a few exceptions, this structure is conserved in almost all bacterial SSBs[25]. Each monomer is composed of two domains: (i) an N-terminal domain of SSB forms a classic oligonucleotide / oligosaccharide-binding (OB) fold responsible for ssDNA binding, and (ii) a flexible C-terminal domain (C-domain) composed of the intrinsically disordered linker (IDL) which ends with a conserved motif, often termed “acidic tip” (C-tip), responsible for the interaction of SSB with other proteins[13,20,26].

The SSB tetramer can bind ssDNA around OB folds in multiple binding modes, among which the best studied are $(SSB)_{35}$ and $(SSB)_{65}$. As the subscripts indicate, in

these modes two or four OB folds bind approximately 35 and 65 nucleotides, respectively.

The preference of the binding mode depends primarily on the concentration and type of salt as well as on the ratio of protein to ssDNA[27–29]. Mode $(SSB)_{65}$ is preferred at a high salt (HS) concentration (>200 mM NaCl or >10 mM $MgCl_2$) and low SSB to ssDNA ratio. In this mode, only limited cooperativity between adjacent tetramers occurs[28,29], where SSB can diffuse along ssDNA, allowing other proteins to bind to the DNA[30]. However, the highly cooperative binding also occurs in the $(SSB)_{65}$ binding mode, even at HS concentrations but in a solution containing glutamate. Since this is a physiologically relevant anion[31], the obtained result suggests an important role for this type of binding *in vivo*[32,33].

The mode $(SSB)_{35}$ is favored at low salt (20 mM NaCl or <1 mM $MgCl_2$) and high SSB to ssDNA ratio where long protein clusters are formed[34,35] and high cooperativity occurs[27,36]. In this mode, redistribution of SSBs via direct transfer occurs rapidly, which is important for SSB recycling during replication[37].

Unlike the ssDNA binding domain (DBD), the IDL region is disordered even when EcSSB is bound to ssDNA[38]. In contrast to C-tip, the IDL region is significantly less conserved among bacterial SSBs and varies in amino acid (aa) content and length (~25-130 aa)[20,39,40]. While at moderate salt concentration, the C-tip inhibits ssDNA binding affinity[26], the IDL region of EcSSB plays the most prominent role in the regulation of inter-tetrameric cooperative binding[20]. Noteworthy, the C-tip[20], as well as additional residues within the DBD that form a "bridging interface" connecting adjacent SSB tetramers[41] also affect cooperativity, but not to the same extent as the IDL region. Namely, replacing this region with a highly charged IDL from *Plasmodium falciparum* SSB protein or deleting the entire IDL while preserving

the acidic tip completely abolished SSB cooperative binding[20]. Also, IDL has been proposed to form separate liquid-liquid phase (LLPS) condensates that provide various functional advantages to cells exposed to stressful growth conditions[42,43]. Detailed analysis of the IDL region identified three proline-rich motifs (PXXP) and multiple hydrophilic GGX repeats that provide flexibility to this region[44]. The authors proposed that the PXXP motifs mediate binding to the OB fold of other SSBs, thus contributing to cooperative binding and that SSB uses the same mechanism to bind the other SIP proteins[18,39,44]. However, the latest results of Keck et al.[45], by analyzing the same interacting partners but using different approaches, showed that PXXP motifs and the length of the IDL region are not important for RecG/SSB interactions. In addition, removing the IDL region did not have a major impact on cell growth except for bacteria that were exposed to stress[20,45,46]. Thus, the IDL regions' role still remains unclear and further research is needed to better understand how it contributes to the functionality of EcSSB especially under unfavorable growth conditions.

Unlike *E. coli*, which contains one SSB protein, many taxonomically diverse groups of bacteria carry on their genome additional copies of *ssb* genes encoding for paralogous SsbBs[47–50]. Although SsbBs retain the highest similarity with the DBD of SsbA proteins they might exhibit different ssDNA binding properties[6,33,47,51,52]. As for the C-terminus of SsbBs, this domain is often reduced in paralogous proteins[47,49,51,53]. Unlike SsbA proteins which have vital roles in DNA metabolic processes, SsbBs are not absolutely required for cell survival. Their biological roles remain largely unexplored and have only been described in a few bacterial species[47,54–57]. In Actinobacteria, obtained results for *Mycobacteria smegmatis* indicated a role of SsbB in recombination repair during

stress[33] while in *S. coelicolor*, it has been shown that SsbB has a key role in chromosomal segregation during sporulation[49].

.

In this study, we examined the influence of the C-terminal domain on the function of the paralogous proteins SsbA and SsbB in the multicellular bacterium *S. coelicolor*, a model for industrially important streptomycetes. Microscopic analysis of mutant strains producing SsbA with altered C-domains led to changes in bacterial growth, aberrant chromosome segregation and irregular septation during the reproductive phase, as previously shown for SsbB. Using a number of different biophysical and biochemical methods, our results revealed that mutations of the C-terminal domains affected the biophysical properties of these proteins and altered the ssDNA binding affinity, clearly indicating the importance of these domains for protein functions.

Results and discussion

SsbA and SsbB from *S. coelicolor* show the most pronounced differences in their C-terminal domains

S. coelicolor is a member of the Actinobacteria and a model organism for studying bacterial differentiation and production of metabolites of medical interest. As the majority of analyzed bacteria belonging to this phylum[49], *S. coelicolor* has two SSB proteins designated, SsbA (199 aa) and SsbB (156 aa). These proteins share an overall sequence identity of 29%, mostly conserved in their N-terminal domains (39.5%) consisting of the first ~120 aa forming a common OB-fold responsible for ssDNA binding. Accordingly, the crystal structures of SsbA and SsbB also showed significant similarities between their OB folds in monomer units with some characteristic details that most likely contribute to their stability[49,58,59]. In contrast,

the C-domains of these proteins differ significantly (Figure 1) and thus show low level of identity (13.8%). However, in both proteins, the C-domain is intrinsically disordered (IDL) and, as in all solved crystal structures of bacterial SSB proteins, this domain is not visible in SsbA and SsbB[7,49]. The C-domain of SsbA comprises 80 aa, among which glycine are the most abundant (~56%), indicating its great flexibility[60], and like EcSSB[13] has an acidic tip (Figure 1). In contrast, the C-domain of SsbB is much smaller (46 aa), does not have an acidic tip and contains many prolines (~24%). Proline residue has a unique cyclic structure compared to other amino acids, which affects the protein structure, it induces a bend into the amino acid chain and contributes to its rigidity[61,62]. Thus, the increased proline content can also be predicted to significantly impact on the local structure of the C-domain of the SsbB protein[39].

Figure 1. Protein sequences of SsbA and SsbB C-domains and their mutant variants. The C-tip (DEPPF) is conserved in the SsbA protein and is shown in red. The C-domain of SsbA is enriched with GGX motifs, the ones mutated in this study are marked in grey. Mutations G/A or P/A are underlined in red. The pseudo-PXXP motifs found in SsbB are marked in yellow. Deleted amino acids are indicated in parentheses.

The recent identification of PXXP motifs within the IDL regions of EcSSB proteins and the proposed role of these motifs in mediating SSB interactions[17,18,44,63] prompted us to inspect in detail the IDL region of SsbA and SsbB proteins. Interestingly, the C-domains of SsbA and SsbB share a higher identity with the C-domain of EcSSB (65 aa) than with each other, 28% and 16.7%, respectively. Although no variations of the PXXP motifs previously reported for EcSSB were found in SsbA[39], there are plenty of GGX repeats identical to EcSSB[44], such as GGG, GGA, GGQ, and GGW (Figure 1). On the other hand, the C-domain of SsbB has only a few glycine residues (4/56) but has two pseudo-PXXP motifs (Figure 1).

Partial deletions of Ssb C-terminal domains have profound impact on *Streptomyces* development

Previously, we have demonstrated that SsbB has a key role in DNA segregation during sporulation of *S.coelicolor* [49]. We have also shown that *ssbBΔC* encoding SsbB119 cannot suppress the defect in chromosome segregation in a *S. coelicolor* strain lacking the wild-type SsbB protein[49]. On the other hand, SsbA was indispensable for the survival of *S. coelicolor*. In this study, we constructed SsbA mutants lacking parts of the C-terminal region. Interestingly, the percentage of revertants to wild type was much higher than expected (90 %), indicating the importance of this regions for the cell fitness. Finally, we succeeded in obtaining two strains, ScSsb162 and ScSsbΔDEPPF while strain ScSsbB121 producing ssbA without C-terminal domain (Figure 1) was lost during strain propagations in several independent experiments which suggests the importance of this domain for SsbA functionality that is essential for a cell survival. Macroscopic analysis also confirmed

morphological changes during sporulation phase of other *S. coelicolor* SsbA mutant strains (Figure S1). Strain ScSsb162 showed slower growth of Ssb162 mutant while SsbΔDEPPF mutant exhibited significantly faster sporulation on MS growth media (Figure S1 A). In addition, mutants grown on rich medium (R5) also showed changes in the pigment production (Figure S1 B). Thus, the morphology of mutant strains was examined in detail by confocal microscopy and compared to wild-type (Figure 2). As shown, ScSsbAΔDEPPF and ScSsbA162 strains had similar defects in chromosome distribution and irregular septation during sporulation phase (Figure 2). This result clearly showed that only complete C-terminal domain assures biological role of SsbA protein. Interestingly, deletion of the acidic tip (the last 10 aa) of *E. coli* SSB, the model protein for studying bacterial SSB proteins, was lethal for bacterial cells [46]. As far as we know, in addition to our result, it has only been reported for the *B. subtilis* that removal of the C-tip of SsbA is not lethal to the bacterium [12]. Unlike *E. coli*, *B. subtilis* and *S. coelicolor*, have two paralogous proteins, SsbA and SsbB. We hypothesize that parologous SsbB protein at least partially suppresses defect in SsbA protein and helps bacteria survive at least under laboratory culture conditions. Given all above, to better understand the function of the C-domain in *S. coelicolor*, in this study we focused on the analyzing the biochemical and biophysical properties of SsbA and SsbB proteins and their variants with altered C-domains.

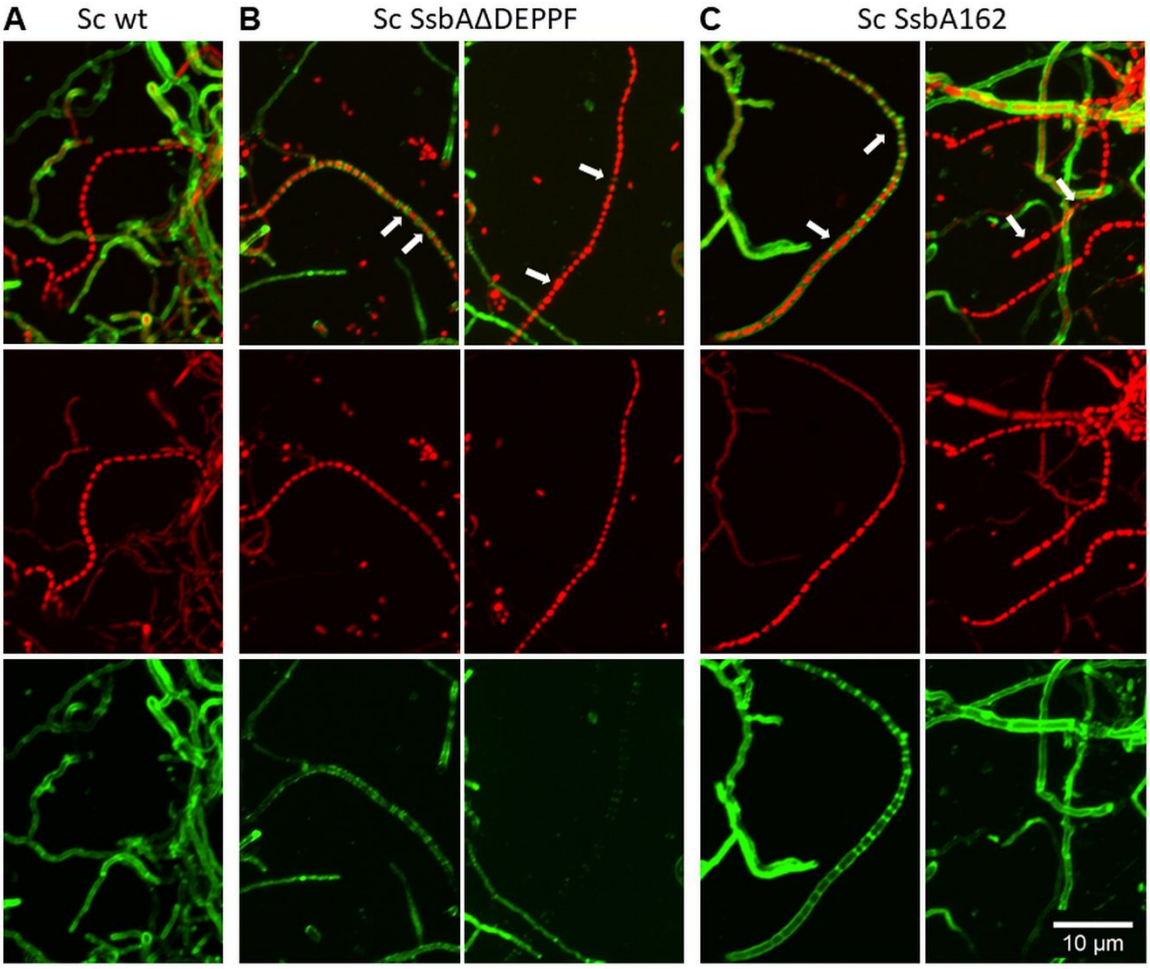

Figure 2. Confocal microscopy images of *S. coelicolor* wild type (A) and strains expressing SsbA protein with mutated C-terminal domain (B and C), as indicated. White arrows indicate different abnormalities in DNA distribution and irregular septation. Upper panels represent merged channels, middle panels DNA stained with propidium iodide while bottom panel cell wall stained with WGA staining. Mycelium was grown for 72h and stained as described in Materials and Methods. Bar= 10 µM, applicable to all images.

The SsbA and its variants with altered C-terminal domain have the potential to form liquid-liquid phase separation

The EcSSB protein was recently reported to form dynamic liquid-liquid phase separation (LLPS) condensates (also known as biomolecular condensates or membrane less organelles) proposed to increase bacterial fitness under varying physiological conditions[42,43,64]. It was also shown that the EcSSB-IDL region is required to form LLPS. Computational analysis performed on a more extensive set of SSBs (717 sequences from 15 major bacterial phylogenetic groups) using a stringent threshold predicted LLPS propensity for ~ 70% of SSBs[42], suggesting the importance of this property for the function of these proteins. The SsbA from *S. coelicolor* (UniProt AC, Q9X8U3) was among the analyzed SSBs and scored positive with both used methods, whereas SsbB (UniProt AC, Q9KYI9) was excluded due to its significantly shorter C-domain. We also performed computational analysis using three different methods, PLAAC[65], CatGranule[66] and PSscore[67] to examine the impact of introduced mutations in the IDL region for predicted LLPS propensity of generated SsbA variants (Figure 1). Three predictors were used for this analysis since they account for different features of the protein and in combination are very useful for predicting LLPS propensity[42,68]. Also noteworthy, PLAAC was originally designed to predict prion-like domains (PrDs), but has been shown to be a good predictor of LLPS[68] since PrDs can form liquid-liquid phase separations. All three algorithms consistently detect the IDL region in SsbA and its variants as a region prone to LLPS formation but also show that targeted mutations affect the propensity of the LLPS region in each variant, albeit differently. Only SsbA121, which lacks almost the entire IDL region but retains the C-tip and SsbB protein score zero for LLPS (PrD) propensity (Figure 3, Figure S2).

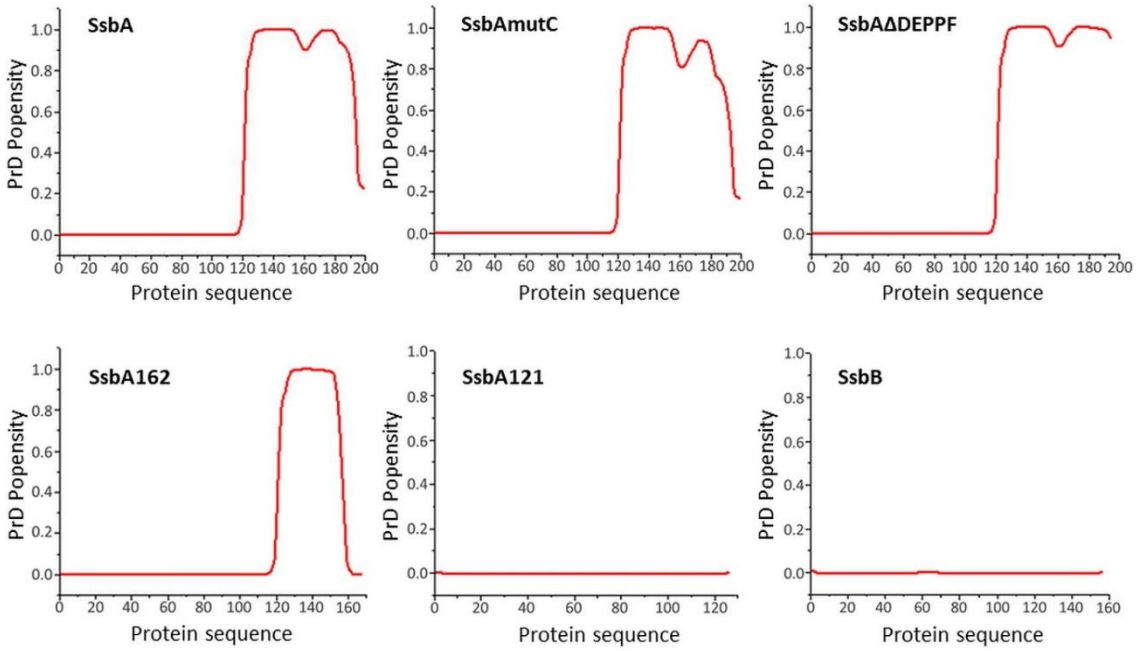

Figure 3. The PrD/LLPS propensity profile for SsbA, its variants and SsbB protein. The residues (shown in red) above the threshold value zero are those predicted by PLAAC and the other two algorithms (Figure S2) with a propensity for PrD/LLPS. The SsbA, and variants marked on the graph show different PrD/LLPS profiles in accordance with the introduced mutation. The SsbA121 without IDL region and SsbB score zero for LLPS propensity.

As reported, the EcSSB condensates formed a turbid solution due to the light scattering on particles with a diameter larger than the wavelength of visible light[42]. Similarly, we observed that SsbA and all variants except SsbA121 at a protein concentration of ~ 1 mg/mL and in low salt (LS) buffer (30 mM NaCl) at RT formed a turbid solution. Since only SsbA is essential for survival[49], it is not surprising that it has the potential to form LLPS condensates that allow bacteria to store increased amounts of SSB in cells and respond rapidly to DNA damage[43]. In contrast to EcSSB, SsbA proteins with IDL region also formed turbid solution in HS buffer (300

mM NaCl), but only at 4 °C. Dynamic Light Scattering (DLS) profile of SsbAΔDEPPF sample was presented as an example of this phenomenon (Figure 4) since it shows that the formation of condensates does not depend on the C-tip, as proposed by Kovács *et al*[42] and which is known to make transient contacts with the OB folds[69], that could contribute to the formation of protein assemblies. This process was reversible as an increase in temperature resulted in a loss of turbidity. DLS analysis (Figure 4A) showed that the peak which corresponds the SsbAΔDEPPF tetramer (D_H ~12 nm, Table 1) is not visible at 4 °C, while much larger particles were formed that contributed to the turbidity (Figure 4B). Also, as the temperature rises, the proportion of tetramers in the solution returns to the initial level (Figure 4A). Repeated temperature changes eventually lead to the formation of insoluble aggregates. Altogether, obtained results support the *in silico* prediction that wild type SsbA has potential to form LLPS condensates. As stated, a protein lacking IDL region (SsbA121) showed no turbidity and did not change DLS profiles at different temperatures (Figure S3), which is in line with results reported for the EcSSB[42] and confirms the importance of the entire IDL region for this process. Consistent with *in silico* prediction, SsbB did not produce turbidity under all tested conditions.

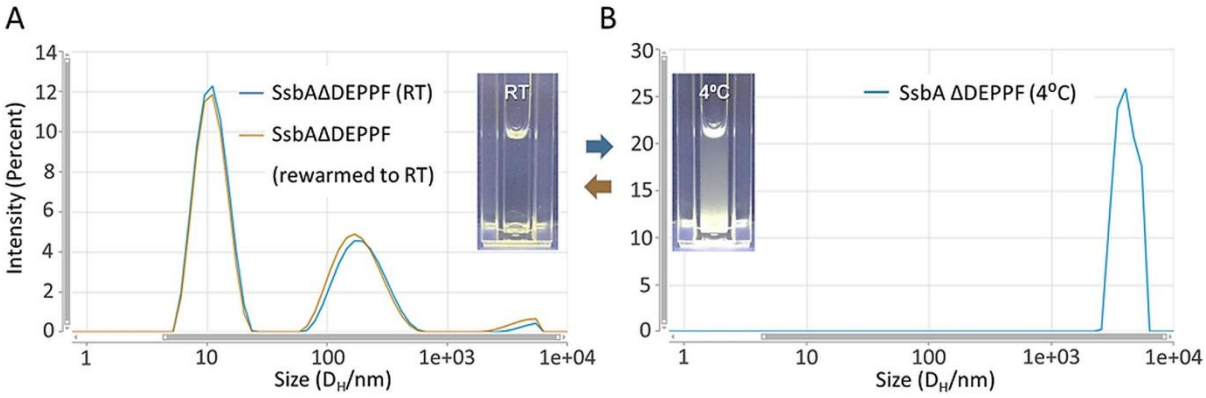

Figure 4. The size of protein particles detected by DLS changes depending on the temperature. A) DLS profiles of the SsbAΔDEPPF sample in buffer containing

300 mM NaCl performed at RT, and after cooling and rewarming the sample to RT, as indicated on the graph. **B)** DLS profile of SsbAΔDEPPF in HS buffer at 4 °C.

Despite their molecular weight differences, SsbA and SsbB show very similar hydrodynamic diameters

The Stokes radii (R_S or Hydrodynamic radii, R_H) of EcSSB and variants with truncated C-domain, SSBc (Δ42 aa) and SSBτ (Δ62 aa), determined by size exclusion chromatography were 3.9 nm, 3.0 nm and 2.7 nm, respectively[70]. Recently analyzed hydrodynamic properties have predicted the globular nature of EcSSB IDLs and showed that R_H decreases with decreasing IDL length[20]. We used the DLS method to assess the hydrodynamic properties of SsbA and SsbB and their IDL variants (Figure 1). Compared to the D_H of the EcSSB protein (7.8 nm in 100 mM NaCl)[70] both SsbA and SsbB, showed a larger D_H measured at a similar salt concentration (150 mM, Table 1). Given the molecular weight (M_w) of these proteins (SsbB<EcSSB<SsbA), the differences in their diameters could be attributed to variability in quaternary structures since the EcSSB has a spheroidal shape, while SsbA and SsbB are more ellipsoidal[38,49,59]. However, SsbA and SsbB, which differ in M_w, mostly due to their C-domains, show negligible differences in their D_Hs (Table 1). This was unexpected since shortening the length of IDL resulted in decreasing D_H of EcSSB[20]. Thus, we assumed that different properties of aa in the SsbB IDL region contribute to the size of its D_H. To better understand the hydrodynamic properties of SsbA and SsbB IDL regions, we measured D_H for all variants at two different salt concentration (150 and 300 mM NaCl). Only SsbB119, which lacks a large part of the C-domain (Figure 1), was omitted from further

analyses since it mostly aggregated already during purification (Figure S4). We also did not perform DLS measurements at LS concentrations because all proteins showed a tendency to aggregate to a different extent. Nevertheless, our results clearly show that deletions or mutation of the IDL regions led to a significant decrease in D_H for all variants, at higher salt concentration (Table 1, Table S1) following the trend reported for EcSSB[20,70]. However, by reducing the salt concentration (150 mM NaCl), the decrease in D_H was the most prominent for wild type Ssb proteins and SsbA121. Considering the structure compaction of the EcSSB IDL region at LS[20] and the fact that SsbA and SsbB behave similarly, it can be concluded that their IDL regions also show a preference to adopt a compact globular conformation[71]. However, while the IDL variants of the EcSSB showed a similar trend to their wild type protein in a LS buffer, the opposite was observed for SsbA and SsbB variants. The D_H of SsbAΔDEPPF, SsbA162, SsbAmutC and SsbBmutC at moderate salt concentration remain largely the same (Table 1, Table S1), indicating disruption of intrinsic interactions between the C-domain and the tetrameric core as a consequence of the introduced mutations in the IDL region.

Table 1 DLS measurements of hydrodynamic diameters of studied Ssb proteins at different salt concentrations. Errors are shown as S.D., whereas statistical significance was confirmed by the t-test (Table S1).

Protein	***T* / °C**	**[NaCl]/mM**	**D_H / nm**	**[NaCl]/mM**	**D_H / nm**
SsbA	25	150	11.08 ± 0.25	300	12.26 ± 0.24
SsbAΔDEPPF	25	150	11.68 ± 0.09	300	11.68 ± 0.21
SsbAmutC	25	150	11.15 ± 0.17	300	10.75 ± 0.14
SsbA162	25	150	9.96 ± 0.38	300	10.13 ± 0.24

SsbA121	25	150	8.31 ± 0.02	300	9.53 ± 0.22
SsbB	25	150	10.63 ± 0.23	300	12.06 ± 0.77
SsbBmutC	25	150	10.50 ± 0.26	300	10.62 ± 0.17

The DLS also detected the presence of additional particles of larger size (≥ 100 nm) in all Ssb protein samples measured at different salt concentrations (Figure S5). As reported, such particles most likely correspond to “start aggregates” at the initial stage of aggregation[72]. Aggregation tendency has already been described for EcSSB protein in numerous cases[4,69,71,73,74]. Accordingly, SsbA showing more similarity to EcSSB, especially in its C-domain compared to SsbB, is also more prone to aggregation suggesting that the C-domain contributes to this process.

Thermally stable Ssb proteins differ in the unfolding enthalpy depending on the size and flexibility of the C-terminal domain

We used differential scanning calorimetry (DSC) to assess the thermal stability of the two *S. coelicolor* paralogous Ssb proteins and their corresponding variants (Figure 1). Both proteins form ellipsoidal tetrameric structure, similar to mycobacterial SSB proteins[50,75–77]. While SsbA has, as in all mycobacterial SSBs, a clamp-like structure that links two monomers, in SsbB, two S-S bridges were found between two monomers[49,59]. Nevertheless, the clamp in SsbA and the disulfide bridges in SsbB have been proposed to contribute to tetramer stability, although we speculated that the formation of S-S bridges is regulated by oxidative stress in *S. coelicolor.* Also, calculations of the free energy of the tetramer dissociation (ΔG_{diss}) predicted higher stability for SsbB tetramer[49]. Despite our predictions, we found that the T_m

of SsbA was 6 °C higher than the T_m of SsbB, needing higher temperatures, more kinetic energy to unfold/melt. Similar experimental results were obtained for *M. tuberculosis* Ssb paralogs[33], where differential scanning fluorimetry was used to evaluate the thermal unfolding. The unfolding temperature, T_m, of MsSSBa was 9 °C higher than MsSSBb. Although the T_m was lower, the transition from folded to unfolded state is a slower and less cooperative process in SsbB. Consequently, the molar enthalpy of this transition is somewhat higher for SsbB than SsbA. The deletions (SsbAΔDEPPF, SsbA162, SsbA121) have not considerably influenced thermal stability. Their impact on the molar enthalpies of the transition was much more pronounced, showing higher ΔH values compared to the wild type SsbA. Considering that the deletions took part in the IDL regions of SsbA protein, where intramolecular non-covalent interactions are not evident, both results are expected, as the M_w of the protein is reduced, while the number of non-covalent bonds, which need to be broken-down, stays the same. Introduced substitutions (SsbAmutC and SsbBmutC) similarly had a low impact on thermal stability, but their effect on the enthalpy of the unfolding is different. Here, the M_w and the number of non-covalent bonds forming the secondary structure motifs are almost identical. Still, the flexibility of the IDL region in mutated SsbA and SsbB proteins is likely altered. The thermodynamic profile of the unfolding transition indicates that the flexibility of the IDL region is significant for the tertiary structure, and there is some interaction between the IDL region and OB fold[71] or other parts of the protein, which diminishes with the loss of flexibility. The absence of this interaction results in lower ΔH for mutC variants. Table 2 shows the unfolding temperatures (T_m) and molar enthalpy changes of the unfolding transitions (ΔH / kJ mol^{-1}), while Figure 5 shows fitted thermograms.

Table 2 Thermal stability data from DSC scans

Protein	T_m / °C	ΔH / kJ mol^{-1}
SsbA	69.16	458.3
SsbAmutC	69.48	405.8
SsbAΔDEPPF	69.35	470.2
SsbA162	70.86	825
SsbA121	69.47	490.7
SsbB	63.12	471.4
SsbBmutC	63.59	452.3

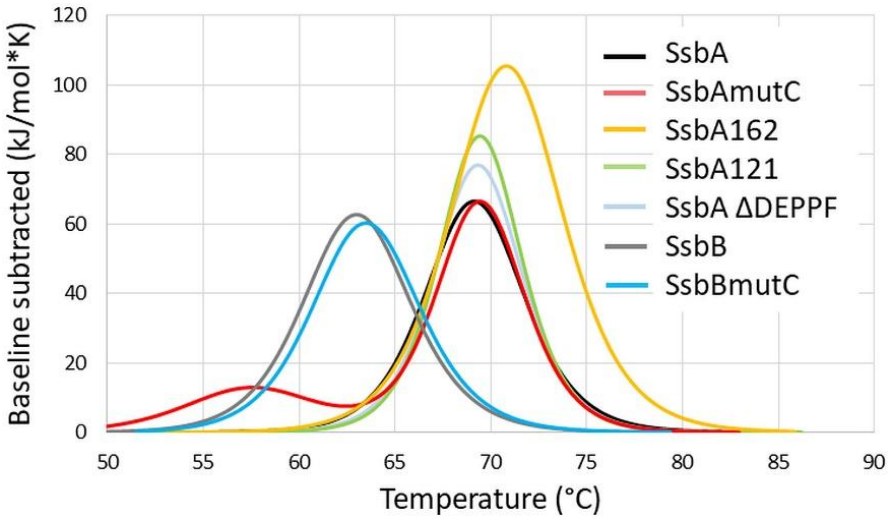

Figure 5. Differential scanning calorimetry thermograms of paralogous Ssb proteins and their variants.

Loss of conformational dynamics of the IDL region upon ssDNA binding

In a quest for more insight into the nature of Ssb affinity towards ssDNA binding, we used ITC to assess this interaction to gain information on the binding

thermodynamics. Regardless of the introduced mutations, the affinities of the proteins remained high. In terms of K_D values they are in the nanomolar range (10^{-9}-10^{-10} M) in LS (30 mM NaCl) conditions, while in higher ionic strength buffer (300 mM) they exhibit submicromolar (10^{-7}-10^{-8} M) affinities. In both conditions, SsbA paralog binds dT_{45} ssDNA more profoundly than SsbB. However, SsbB shows higher affinity with a shorter dT_{35} sequence than SsbA[49] (Table S2) but only at LS. The titrations in HS with dT_{35} showed affinities bellow the experimental sensitivity threshold and could not be determined. Thus, all experiments were performed with dT_{45}. Since the OB-fold, where ssDNA is bound, remained intact in all the mutated proteins, significant deviations in binding affinities were not expected. ITC titrations were used to evaluate small differences in binding caused by changes introduced in the IDL region of the protein. An intriguing difference can be observed with the SsbAΔDEPPF, where in LS conditions protein exhibits the lowest affinity for dT_{45} binding, while in HS conditions same mutated protein shows the highest affinity for the ssDNA. In the HS conditions charged amino acid residues, of the SsbA, SsbB and their mutated C-domains, with exception of SsbAΔDEPPF, are saturated with counterions via salt bridges. Thus, rendering the proteins' affinity for ssDNA interaction, somewhat lower than in the case of more neutral end of the variant lacking the acidic DEPPF tip. In the case of SsbAΔDEPPF, van der Waals (vdW) contacts have more influence on the binding thermodynamics[78]. Unlike the EcSSB ΔC8 which at LS shows the same binding affinity as EcSSB[26], SsbAΔDEPPF showed lower binding affinity (Table 3) indicating that the electrostatic interactions are much more prominent in lower ionic strength buffers, where charged tip can seize the best position to accommodate ssDNA binding. The binding of ssDNA with all the studied Ssb proteins is totally under enthalpic control (Table 3). Entropic

contribution to the binding thermodynamics is overcompensated with the entropic penalty due to the proteins' loss of conformational dynamics. The entropic penalty is extremely high, indicating considerable conformational mobility and numerous degrees of freedom[71]. Binding is driven by enthalpic contributions, already mentioned vdW contacts, hydrogen bonding and electrostatic interactions, which contribute to the binding free energy (ΔG).

Table 3 Thermodynamical characteristics, stoichiometry and binding affinities of Ssb proteins for dT_{45} in LS and HS buffer formulations.

Protein	***I*c/mM**	***N***	**K_D/M**	**ΔH/kJ mol^{-1}**	**ΔG/kJ mol^{-1}**	**$-T\Delta S$/kJ mol^{-1}**
SsbA	30	0.82	4.21E-10	-239.5	-53.6	185.5
SsbAmutC	30	0.71	9.815E-10	-274.5	-51.6	223.0
SsbA162	30	0.75	6.365E-10	-271.0	-52.7	218.5
SsbA121	30	0.71	6.01E-10	-337.0	-52.7	284.0
SsbAΔDEPPF	30	0.64	1.56E-09	-267.5	-50.4	217.5
SsbB	30	0.72	6.59E-10	-325.0	-52.5	272.0
SsbBmutC	30	0.75	5.63E-10	-330.0	-52.9	277.0
SsbA	300	0.67	1.755E-07	-230	-38.6	191.5
SsbAmutC	300	0.83	1.054E-07	-254	-40.6	213.7
SsbA162	300	0.73	1.33E-07	-226.5	-39.3	187.5
SsbA121	300	0.70	7.08E-07	-140	-35.1	105
SsbAΔDEPPF	300	0.64	7.06E-08	-207.5	-40.85	166.5
SsbB	300	0.77	6.43E-07	-262	-35.4	227
SsbBmutC	300	0.63	1.74E-07	-285.5	-38.65	246.5

We also used CD spectroscopy, as described in Supplemental Information, to evaluate the secondary structure of the studied proteins and changes induced by ssDNA binding. However, only the SsbA162 and SsbA121 show a reliable correlation between fitted and experimental data (Figure S6, Table S3), confirming the importance of the full length IDL and its overlap with the OB fold in the 3-D space. For other proteins, the discrepancies between the model and raw CD spectra allow a general discussion of trends but offer no confirmations of the structure.

The IDL region of both Ssb proteins regulate their cooperative binding

IDL is crucial for inter-tetramer SSB cooperative binding to ssDNA. It was previously shown[20] that complete removal of the IDL or significant changes in its amino acid composition eliminates highly cooperative binding to ssDNA. In this study, we used the qualitative method, EMSA to assess the contribution of the C-domains of SsbA and SsbB proteins to cooperative ssDNA binding. Since cooperative ssDNA binding was also affected by the IDL length and by the C-tip[20], we also examined all Ssb variants with altered C-domains. Only SsbAΔDEPPF lack the C-tip, SsbAmutC has a mutated IDL, while SsbA162 (Δ 32 aa) and SsbA121 (Δ 73 aa) have a truncated C-domain (Figure 1). In addition, we examined SsbB since it naturally has a shorter C-domain than SsbA, as well as its mutated variant, SsbBmutC. Note that we did not examine SsbB119 due to the aforementioned problem with aggregation. As shown in Figure 6 all examined proteins, except for SsbA121 which lacks complete IDL region but retain C-tip, showed bimodal distribution of ssDNA, characteristic of cooperative ssDNA binding. This is due to the non-random binding of Ssb proteins to ssDNA, which leads to the appearance of a population saturated with protein and another population with little or no protein bound[28]. The EMSA showed that, despite their

quite different C-domains, both proteins, SsbA and SsbB form cooperative nucloprotein clusters (Figure 6). More globular structure of the IDL region is important for cooperative binding[7]. Described hydrodynamic properties (Table 1) of these proteins predicted that IDLs of SsbA and SsbB occupy more globular conformations. However, in comparison to SsbA, the SsbB shows low to moderate cooperativity because at a higher protein-to-ssDNA ratio (*R* 0.06 - 0.09) there is still a lot of unbound ssDNA together with randomly bound and saturated ssDNA. As shown, increasing the protein concentration leads to the fast saturation of ssDNA, and the appearance of higher molecular mass complexes that migrate more slowly (Figure 6B). In contrast to the wild-type protein, the SssBmutC protein shows more cooperative binding, similar to that of the SsbA protein, suggesting that the IDL region also plays an important role in regulating cooperative binding for this protein.

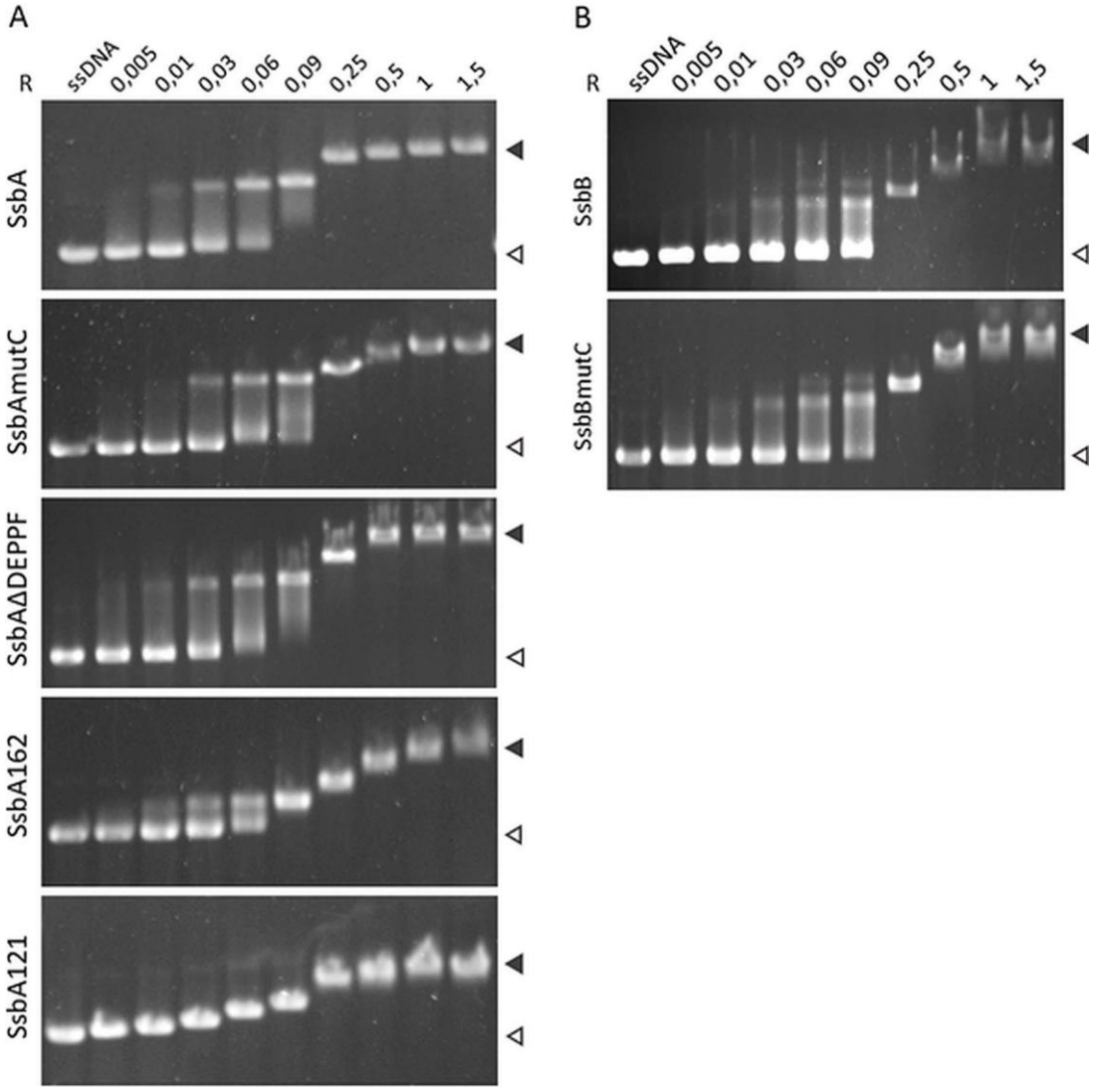

Figure 6. Cooperativity of SsbA and SsbB and their variants bound to Phi X174. EMSAs of SsbA **(A)** and SsbB **(B)** complexes formed with Phi X174 ssDNA at RT and different protein-to-DNA ratios (*R*) as described in Materials and methods and indicated above the lanes. Both proteins show a bimodal distribution of bound ssDNA at various ratios (*R*). indicating moderate (SsbB) and highly cooperative (SsbA) binding (R_{35} is calculated as described in Materials and methods). Except for SsbA121, which only shows a single band indicating no cooperativity, all other SsbA variants as well as SsbBmutC show electrophoresis patterns similar to wild type SsbA. Unbound ssDNA is shown by a white triangle, whereas black triangle indicates saturated ssDNA.

Conclusions

The analyzes carried out in this study confirmed that very different C-domains of paralogous SsbA and SsbB proteins participate in regulating their biophysical properties and, consequently, biological functions in S. coelicolor, a model bacterium of industrially important streptomycetes. Microscopic analysis showed that strains producing SsbA protein with truncated C-terminal domain exhibited different abnormalities in DNA distribution and irregular septation during sporulation. DLS showed that only SsbA, which is essential for survival, has the potential to form LLPS condensates and store increased amounts of SSB in cells in membrane-less organelles. In our study, this phenomenon depended on the C-terminal domain but not on its acidic C-tip, as previously suggested. Additionally, biophysical analysis showed hydrodynamic properties of all protein variants, implying that disordered C-domains of SsbA and SsbB occupy more globular conformation. Despite differences in molecular weight, SsbA and SsbB have similar DH, likely due to the properties of their aa composition in Ssb C-domains. With unfolding temperatures around 70 °C, SsbA is thermally more stable than SsbB, which has 6 °C lower Tm. Shortening the C-domain increases, while mutation of this domain causes the decrease of the molar unfolding enthalpy. Although the entropic penalty is huge due to the loss of conformational mobility, the binding affinity towards ssDNA of all the studied Ssb proteins remains immense. This tight binding is driven by Van der Waals contacts, hydrogen bonding, and electrostatic interactions. EMSA showed that the C-domain is crucial for a high cooperative binding of SsbA and also suggested that the C-domain may have an important role in regulating the cooperative binding of SsbB.

Materials and methods

Enzymes, Reagents and DNA

All solutions were prepared with reagent grade chemicals and Milli-Q water. EmeraldAmp GT PCR Master mix was from Takara. Miniprep Kit, Gel Extraction Kit, PCR Purification Kit and Ni-NTA agarose were from Qiagen. Fast Digest restriction enzymes (Table S4), T4 DNA ligase, lysozyme and SYBR Gold were from Thermo Fisher Scientific. Deoxyribonuclease I, agarose, tryptone, yeast extract, bacteriological agar, ampicillin salt, disodium phosphate (Na_2HPO_4), monosodium phosphate (NaH_2PO_4), Tris-base, Coomassie Brilliant Blue R-250, sodium dodecyl-sulfate (SDS), 1,4-dithiothreitol (DTT), ethylenediaminetetraacetic acid (EDTA), glycine, N,N,N′,N′-Tetramethyl ethylenediamine (TEMED), 2-mercaptoethanol and ethidium bromide (EtBr) were purchased from Sigma-Aldrich. Isopropyl β-D-1-thiogalactopyranoside (IPTG) was from Carl Roth. Sodium chloride (NaCl), acetic acid (CH_3COOH), hydrochloric acid (HCl), glycerol and isopropyl alcohol were from Kemika (CRO). Imidazole, sodium acetate (CH_3COONa) and ammonium persulfate (APS) were from Merck. 40% Acrylamide/bis solution was from Bio-Rad.
All primers (Table S4) used for cloning experiments and oligonucleotide dT_{45} in concentration of 0.2 μmol with extinction coefficient ε= 396 mL/μmol, used in DNA binding assays were purchased from Macrogen's oligo synthesis service. Phi X174 Virion DNA (5386 nt) in concentration of 1 mg/mL was purchased from New England BioLabs. All genetic constructs were verified by Sanger sequencing (Macrogen). The Clustal Omega was used for carrying out pairwise (PSA) or multiple alignments (MSA) of nucleotide sequences.

Genetic constructs and cloning

Plasmids, pQE-*ssbA* and pQE-*ssbB* containing *his*-tagged *ssb* genes from *S. coelicolor* (*ssb*A, SCO3907 and *ssbB*, SCO2683) obtained previously[49,53] were used as a template to generate all *ssb* variants used for in vitro studies (s*sbAmutC*, *ssbA162, ssbA121*, *ssbAΔDEPPF*, *ssbBmutC* and *ssbB119*) encoding for SsbA or SsbB proteins mutated in C-domain. Note that SsbB119 was obtained in previous study and was designated pQEssbBΔC[49]. Genes encoding for *ssbA* and *ssbB* variants were obtained by PCR amplification with SC-A_F and SC-B_F, respectively, and the corresponding reverse primers. Only *ssbAmutC* was generated in two steps as indicated in Table S4. Amplified PCR products were digested with the appropriate restriction enzymes (Table S4) and ligated into PQE-30 vectors. SsbACt, SsbA162 and SsbADEPPF mutant strains were generated for *in vivo* studies (Table S5, Table S6). All positive clones were confirmed by sequencing. Mutants producing SsbA protein with partial deletions of C-terminal domain were prepared using previously developed I-Sce meganuclease protocol[79]. Recombinant pIJ12738 plasmid carrying I-Sce recognition site and flanking regions 1500 nt around deletion sites in SsbA Ct were constructed using standard methods. Flanking regions were amplified using the primers indicated in Table S4, AmpliTaq GOLD (Applied Biosystems), and genomic DNA from *Streptomyces coelicolor* M145. The PCR products of the upstream and downstream flanking regions were digested with appropriate restriction enzymes (FastDigest, Thermo Scientific), upstream with *Xba*I and *Bam*HI and downstream with *Ba*mHI and *Kpn*I. Obtained fragments were ligated together with T4 DNA ligase (Thermo Scientific, EL001), and in the second step, *Xba*I/*Kpn*I-digested plasmid pIJ12738 was added to the reaction. This ligation mixture was transformed into *E. coli* XL1 cells. Positive clones carrying desired in-frame deletion of SsbA Ct were detected by colony PCR and verified by Sanger sequencing.

Positives were transformed into nonmethylating *E. coli* strain ET12567/pUZ8002 and conjugated to *S. coelicolor* according to the protocol described previously[80]. To select the first crossing-over event, in which the recombinant plasmid was integrated through flanking regions, plates were overlaid with apramycin and screened by colony PCR for clones carrying on their genomes wild-type and mutant copies of the *ssbA* gene. Selected clones were grown until sporulation, and plasmid pIJ12742, containing the gene encoding I-Sce meganucelase, was introduced by conjugation with *E. coli* strain ET12567. Exconjugants were selected with thiostrepton. I-Sce meganuclease introduced a double-strand break at a I-Sce recognition site within the integrated plasmid pIJ12738. The surviving colonies that either reverted to the wild-type genotype or had mutant gene copy were analysed by PCR. To induce loss of plasmid pIJ12742, colonies were grown at 37 °C and afterwards verified for loss of apramycin and thiostrepton resistance. Mutant strains were verified by sequencing. The presence of shorter protein variant, SsbA162 in strain ScSsbA162 was additionally confirmed by Western blot using antiSsbA antibiodies and standard procedures.

Bacterial strains and growth conditions

E. coli XL1-Gold was used for cloning, while *E. coli* NM522 was used for over-expression experiments. Both strains were grown on solid Lauria Bertaini (LB) agar plates or in liquid LB medium supplemented with ampicillin (100 μg/mL) because plasmid pQE-30 carries the amp^R gene. The strains were incubated at 37 °C, and when the cells were growing in the liquid, the flasks were shaken at 250 rpm. With one exception, during the over-expression experiment after IPTG induction the temperature for growing *E. coli* NM522 was reduced to 16 °C. For confocal

microscopy, *S. coelicolor* M145, ScSsbAΔDEPPF and ScSsbA162 were grown in the acute angle of sterile coverslips inserted obliquely in MS. After 3 days, the coverslips were removed, and stained using Schwedock protocol [81]

Protein overexpression and purification

Heterologous overexpression was achieved in *E. coli* NM522 transformed with pQE plasmids carrying *his*-tagged wild type *ssb* genes or their mutated variants. The cells were grown at 37 °C to an optical density (OD_{600}) 0.5-0.6 and the expression of the recombinant protein was induced by 1mM of isopropyl-b-D-thiogalactopyranoside (IPTG) as described previously[49] with following modifications. Bacterial cells were growing overnight at 16 °C, biomass were centrifuged for 30 min at 4500 rpm and resuspended in Lysis buffer (50 mM phosphate buffer, pH 7.5, 800 mM NaCl). Lysozyme (0.3 mg/mL) and Deoxyribonuclease I (0.7 mg/mL) was added and bacterial suspension was incubated for additional 30 min on ice. After sonication (3 x 30 s), cell lysate was centrifuged for 30 min at 10000 rpm and supernatant was filtered on 0.22 μm filter. Purification of His-tagged proteins from cell-free extract was achieved by Ni-NTA resin (Qiagen). Column with resin was equilibrated with Lysis buffer supplemented with 40 mM imidazole before cell lysate was passed through the column. Wash buffer (50 mM phosphate buffer, pH 7.5, 300 mM NaCl, 50 mM imidazole) was used to remove unbound or nonspecifically bound proteins and His-tagged proteins were eluted with Elution buffer (50 mM phosphate buffer, pH 7.5, 300 mM NaCl, 300 mM imidazole). Fractions with purified protein were pooled, dialyzed against the appropriate buffer, P1 (50 mM phosphate buffer, pH 7.5, 30 mM NaCl) or P2 (50 mM phosphate buffer pH 7.5, 300 mM NaCl) as needed for further experiments or stored in P2 buffer, SsbA at RT and SsbB at +8 °C no more than

three weeks. When needed proteins were concentrated on centrifugal filter units with 10 kDa M_w cut-off (Amicon Ultra 4 centrifugal filters). To verify protein purity proteins were analyzed on a 12% SDS-PAGE. Concentrations were determined by NanoDrop 2000 (Thermo Fisher Scientific, USA) using extinction coefficients and molecular weight of each protein as shown in Table S7.

Bioinformatics analysis

Protein sequences were aligned in online version of MAFFT v.7 (https://mafft.cbrc.jp/alignment/server/)[82] using the E-INS algorithm which considers multiple conserved domains and long gaps in target sequences; other parameters were left at default values. To predict the liquid-liquid phase separation (LLPS propensity of the SsbA, SsbB and their variants mutated in the IDL region (Figure 1) we used web servers of three predictors which take into account a different set of protein features indicative of LLPS. The PLAAC - prion-like amino acid composition algorithm (http://plaac.wi.mit.edu/) predicts prion-like domains(PrD) based on sequence composition[65]. The PScore algorithm (http://abragam.med.utoronto.ca/~JFKlab/Software/psp.htm) predicts protein propensity for long-range planar pi−pi contacts[67]. The CatGranule algorithm predicts the propensity of proteins to form granules[66]. Default parameters were used for all three predictors.

Dynamic light scattering

DLS measurement was performed in Zetasizer Ultra (Malvern Panalytical) with He-Ne laser in a low-volume quartz batch cuvette (ZEN2112) from three different

angles. The total volume of each sample (40 µL) included the analyzed protein at a final concentration of 1 mg/mL in P2 buffer and in P3 buffer (50 mM phosphate buffer, pH 7.5, 150 mM NaCl). Before starting the DLS analysis, all samples were filtered through a 0.22 µm filter (Merck, Millipore). The measurements were performed at 25 °C using the automatic mode for identifying the best number of subruns and measurement time ($n = 2$). The size of the protein particle (hydrodynamic diameter, D_H) were calculated from the correlation function using the ZS XPLORER software (Malvern Panalytical).

Differential scanning calorimetry

Measurements were performed on Nano DSC, Differential Scanning Calorimeter (TA Instruments). Upon buffer P2 - buffer P2 measurement, used for baseline subtraction, reference cell was filled with P2 buffer and sample cell with protein (1 mg/mL), prepared in P2 buffer. Buffer and protein solutions were degassed under reduced pressure (0.64 bar, 10 min), prior to the measurements. Temperature range was between 20 and 100 °C, with 1 °C/min. Equilibration step was one minute and 6 atm pressure was applied. Raw data was processed in Nano Analyze software (TA Instruments).

Isothermal titration calorimetry

ITC was used to measure the thermodynamic parameters of interactions between different variants of the paralogous Ssb proteins (Figure 1) and ssDNA. Binding affinity and ratio (K_D and N, respectively), the binding enthalpy (ΔH_r) are directly

derived from the equilibrium titration experiment, while entropy, (ΔS_r) and Gibbs energy (ΔG_r) are calculated.

Titrations were performed on MicroCal VP-ITC (Malvern Panalytical, UK). The reference cell was filled with ultrapure water. Experiments were carried out by titrating 1 μM protein substrate solution (SsbA, SsbB and their mutants in P1 or P2 buffer) in the cell with 25 μM oligonucleotide dT_{45} ligand solution in a buffer P1 or P2 from the rotating syringe (220 rpm). Aliquots of the dT_{45} (one aliquot of 2 μL, 18 aliquots of 5 μL and 11 aliquots of 10 μL) were injected into a thermostated cell (25.0 °C) containing 1.4406 mL of the protein. The spacing between the injections was set to 300-360 s, with the initial delay of 2000 s in all the experiments. Prior to the titrations, both solutions were degassed under reduced pressure (0.64 bar, 10 min). Measurements were performed in triplicate for each protein. Origin 7.5 software, supplied by the ITC manufacturer was used for data analysis. Protein concentrations were determined by indirect spectrophotometric methods.

Electrophoretic mobility shift assay

Cooperative binding of SSB proteins to long ssDNA (Phi X-174, 5386 nt) was assessed by EMSA method as described[28,41], with minor modifications. All reactions were prepared in 20 μL of binding buffer (10 mM Tris HCl, pH 7.5, 30 mM NaCl, 0.1 mM EDTA) with a constant amount of ssDNA (0.3 μg) and increasing concentrations of SSB protein as shown in Figure 6. Protein to ssDNA ratios (R_{35}) were calculated [$R = n$ x [SSB (tetramer)/(nucleotide)][28] assuming that the SsbA and SsbB proteins binding site size (n) is ~ 35 nucleotides, since the structurally similar Ssb from *M. smegmatis* has occluded binding site similar to highly

cooperative EcSSB binding[33]. The reaction mixtures were incubated for 20 min at 22 °C, and 4 µL of 50% glycerol was added to each sample before being loaded onto a 0.3% agarose gel. Electrophoresis was performed at 30 V in a running buffer (20 mM Tris HCl, pH 7.5, 0.4 mM sodium acetate, 0.1 mM EDTA) at RT for 3.5 hours. The gel was stained for 30 minutes with SYBR Gold dye diluted in a running buffer (1:20,000). For better visualization of bands, it was necessary to separate SSB proteins from DNA by soaking the gel in a running buffer supplemented with 1 M NaCl for 45 min.

Confocal microscopy

Bacterial strains used in this study were grown as described above. Samples were studied using a Dragonfly confocal microscope system, using 100x/1.47NA HC PL APO oil objective (Leica), iXon Ultra 88 EM-CCD and Sona camera (Andor Technology, Belfast, UK). Images were processed using FIJI[83].

Acknowledgments

The authors thank the company LKB for providing DLS - Zetasizer Ultra (Malvern Panalytical) instrument and Stanislav Martin and Filip Šupljika for helpful advices that contributed to this work. This work was funded by The Croatian Science Foundation, project: IP-2018-01-1754.

Conflict of interest

The authors declare no conflicts of interest.

Author contributions

GP: carried out most of the biochemical experiments, analyzed the data, and help in writing the manuscript; ŽF: helped with carrying out all biological experiments and in writing the manuscript; MĆ: helped with carrying out experiments and analyzing data; TP: helped with carrying out experiments and in writing the manuscript; KZ: helped in writing the manuscript; IC and DV: designed the study, helped with carrying out experiments and analyzing data, oversaw the study and wrote-reviewed and edited the manuscript.

Supporting information

Additional supporting information may be found online in the Supporting Information section at the end of this article.

References

[1] J.W. Chase, K.R. Williams, Single-Stranded Dna Binding Proteins Required For Dna Replication, Annu. Rev. Biochem. 55 (1986) 103–136. https://doi.org/10.1146/annurev.bi.55.070186.000535.

[2] S.C. Kowalczykowski, D.A. Dixon, A.K. Eggleston, S.D. Lauder, W.M. Rehrauer, Biochemistry of homologous recombination in Escherichia coli, Microbiol. Rev. 58 (1994) 401–465. https://doi.org/10.1128/mr.58.3.401-465.1994.

[3] T.M. Lohman, M.E. Ferrari, Escherichia Coli Single-Stranded Dna-Binding Protein: Multiple DNA-Binding Modes and Cooperativities, Annu. Rev.

Biochem. 63 (1994) 527–570.
https://doi.org/10.1146/annurev.bi.63.070194.002523.

[4] R.R. Meyer, P.S. Laine, The single-stranded DNA-binding protein of Escherichia coli, Microbiol. Rev. 54 (1990) 342–380. https://doi.org/10.1128/mr.54.4.342-380.1990.

[5] A.H. Marceau, Functions of Single-Strand DNA-Binding Proteins in DNA Replication, Recombination, and Repair, in: 2012: pp. 1–21. https://doi.org/10.1007/978-1-62703-032-8_1.

[6] K.-L. Chen, J.-H. Cheng, C.-Y. Lin, Y.-H. Huang, C.-Y. Huang, Characterization of single-stranded DNA-binding protein SsbB from Staphylococcus aureus : SsbB cannot stimulate PriA helicase, RSC Adv. 8 (2018) 28367–28375. https://doi.org/10.1039/C8RA04392B.

[7] E. Antony, T.M. Lohman, Dynamics of E. coli single stranded DNA binding (SSB) protein-DNA complexes, Semin. E. Antony, T.M. Lohman, Dyn. E. Coli Single Stranded DNA Bind. Protein-DNA Complexes, Semin. Cell Dev. Biol. 86 102–111. Https//Doi.Org/10.1016/j.Semcdb.2018.03.017.Ars Cell Dev. Biol. 86 (2019) 102–111. https://doi.org/10.1016/j.semcdb.2018.03.017.

[8] M.S. Wold, Replication Protein A: A Heterotrimeric, Single-Stranded DNA-Binding Protein Required for Eukaryotic DNA Metabolism, Annu. Rev. Biochem. 66 (1997) 61–92. https://doi.org/10.1146/annurev.biochem.66.1.61.

[9] I.J. Molineux, M.L. Gefter, Properties of the Escherichia coli DNA-binding (unwinding) protein interaction with nucleolytic enzymes and DNA, J. Mol. Biol. 98 (1975) 811–825. https://doi.org/10.1016/S0022-2836(75)80012-X.

[10] R.R. Meyer, J. Glassberg, J. V Scott, A. Kornberg, A temperature-sensitive single-stranded DNA-binding protein from Escherichia coli., J. Biol. Chem. 255 (1980) 2897–901. http://www.ncbi.nlm.nih.gov/pubmed/6244299.

[11] K. Muniyappa, S.L. Shaner, S.S. Tsang, C.M. Radding, Mechanism of the concerted action of recA protein and helix-destabilizing proteins in homologous recombination., Proc. Natl. Acad. Sci. 81 (1984) 2757–2761. https://doi.org/10.1073/pnas.81.9.2757.

[12] A. Costes, F. Lecointe, S. McGovern, S. Quevillon-Cheruel, P. Polard, The C-Terminal Domain of the Bacterial SSB Protein Acts as a DNA Maintenance Hub at Active Chromosome Replication Forks, PLoS Genet. 6 (2010) e1001238. https://doi.org/10.1371/journal.pgen.1001238.

[13] R.D. Shereda, A.G. Kozlov, T.M. Lohman, M.M. Cox, J.L. Keck, SSB as an Organizer/Mobilizer of Genome Maintenance Complexes, Crit. Rev. Biochem. Mol. Biol. 43 (2008) 289–318. https://doi.org/10.1080/10409230802341296.

[14] Z. Cheng, A. Caillet, B. Ren, H. Ding, Stimulation of Escherichia coli DNA damage inducible DNA helicase DinG by the single-stranded DNA binding protein SSB, FEBS Lett. 586 (2012) 3825–3830. https://doi.org/10.1016/j.febslet.2012.09.032.

[15] C. Petzold, A.H. Marceau, K.H. Miller, S. Marqusee, J.L. Keck, Interaction with Single-stranded DNA-binding Protein Stimulates Escherichia coli Ribonuclease HI Enzymatic Activity, J. Biol. Chem. 290 (2015) 14626–14636. https://doi.org/10.1074/jbc.M115.655134.

[16] S.H. Chen, R.T. Byrne-Nash, M.M. Cox, Escherichia coli RadD Protein Functionally Interacts with the Single-stranded DNA-binding Protein, J. Biol.

Chem. 291 (2016) 20779–20786. https://doi.org/10.1074/jbc.M116.736223.

[17] R. Nigam, M. Mohan, G. Shivange, P.K. Dewangan, R. Anindya, Escherichia coli AlkB interacts with single-stranded DNA binding protein SSB by an intrinsically disordered region of SSB, Mol. Biol. Rep. 45 (2018) 865–870. https://doi.org/10.1007/s11033-018-4232-6.

[18] P.R. Bianco, The mechanism of action of the <scp>SSB</scp> interactome reveals it is the first <scp>OB</scp> -fold family of genome guardians in prokaryotes, Protein Sci. 30 (2021) 1757–1775. https://doi.org/10.1002/pro.4140.

[19] M.K. Shinn, S.K. Chaturvedi, A.G. Kozlov, T.M. Lohman, Allosteric effects of E. coli SSB and RecR proteins on RecO protein binding to DNA, Nucleic Acids Res. 51 (2023) 2284–2297. https://doi.org/10.1093/nar/gkad084.

[20] A.G. Kozlov, E. Weiland, A. Mittal, V. Waldman, E. Antony, N. Fazio, R. V. Pappu, T.M. Lohman, Intrinsically Disordered C-Terminal Tails of E. coli Single-Stranded DNA Binding Protein Regulate Cooperative Binding to Single-Stranded DNA, J. Mol. Biol. 427 (2015) 763–774. https://doi.org/10.1016/j.jmb.2014.12.020.

[21] J.L. Keck, Single-Stranded DNA Binding Proteins: Methods and Protocols, Humana Press, 2012. https://books.google.hr/books?id=85_VuQAACAAJ.

[22] S. Raghunathan, A.G. Kozlov, T.M. Lohman, G. Waksman, Structure of the DNA binding domain of E. coli SSB bound to ssDNA., Nat. Struct. Biol. 7 (2000) 648–52. https://doi.org/10.1038/77943.

[23] S. Chrysogelos, J. Griffith, Escherichia coli single-strand binding protein

organizes single-stranded DNA in nucleosome-like units., Proc. Natl. Acad. Sci. 79 (1982) 5803–5807. https://doi.org/10.1073/pnas.79.19.5803.

[24] S. V. Kuznetsov, A.G. Kozlov, T.M. Lohman, A. Ansari, Microsecond Dynamics of Protein–DNA Interactions: Direct Observation of the Wrapping/Unwrapping Kinetics of Single-stranded DNA around the E.coli SSB Tetramer, J. Mol. Biol. 359 (2006) 55–65. https://doi.org/10.1016/j.jmb.2006.02.070.

[25] E. Antony, T.M. Lohman, Dynamics of E. coli single stranded DNA binding (SSB) protein-DNA complexes, Semin. Cell Dev. Biol. 86 (2019) 102–111. https://doi.org/10.1016/j.semcdb.2018.03.017.

[26] A.G. Kozlov, M.M. Cox, T.M. Lohman, Regulation of Single-stranded DNA Binding by the C Termini of Escherichia coli Single-stranded DNA-binding (SSB) Protein, J. Biol. Chem. 285 (2010) 17246–17252. https://doi.org/10.1074/jbc.M110.118273.

[27] T.M. Lohman, L.B. Overman, Two binding modes in Escherichia coli single strand binding protein-single stranded DNA complexes. Modulation by NaCl concentration., J. Biol. Chem. 260 (1985) 3594–3603. https://doi.org/10.1016/S0021-9258(19)83663-3.

[28] T.M. Lohman, L.B. Overman, S. Datta, Salt-dependent changes in the DNA binding co-operativity of Escherichia coli single strand binding protein, J. Mol. Biol. 187 (1986) 603–615. https://doi.org/10.1016/0022-2836(86)90338-4.

[29] W. Bujalowski, L.B. Overman, T.M. Lohman, Binding mode transitions of Escherichia coli single strand binding protein-single-stranded DNA complexes. Cation, anion, pH, and binding density effects., J. Biol. Chem. 263 (1988) 4629–4640. https://doi.org/10.1016/S0021-9258(18)68829-5.

[30] R. Roy, A.G. Kozlov, T.M. Lohman, T. Ha, SSB protein diffusion on single-stranded DNA stimulates RecA filament formation, Nature. 461 (2009) 1092–1097. https://doi.org/10.1038/nature08442.

[31] B. Richey, D.S. Cayley, M.C. Mossing, C. Kolka, C.F. Anderson, T.C. Farrar, M.T. Record Jr, Variability of the intracellular ionic environment of Escherichia coli. Differences between in vitro and in vivo effects of ion concentrations on protein-DNA interactions and gene expression, J. Biol. Chem. 262 (1987) 7157–7164.

[32] A.G. Kozlov, M.K. Shinn, E.A. Weiland, T.M. Lohman, Glutamate promotes SSB protein–protein Interactions via intrinsically disordered regions, J. Mol. Biol. 429 (2017) 2790–2801. https://doi.org/10.1016/j.jmb.2017.07.021.

[33] A. Singh, M. Vijayan, U. Varshney, Distinct properties of a hypoxia specific paralog of single stranded DNA binding (SSB) protein in mycobacteria, Tuberculosis. 108 (2018) 16–25. https://doi.org/10.1016/j.tube.2017.10.002.

[34] J.D. Griffith, L.D. Harris, J. Register, Visualization of SSB-ssDNA Complexes Active in the Assembly of Stable RecA-DNA Filaments, Cold Spring Harb. Symp. Quant. Biol. 49 (1984) 553–559. https://doi.org/10.1101/SQB.1984.049.01.062.

[35] L. Hamon, D. Pastre, P. Dupaigne, C.L. Breton, E.L. Cam, O. Pietrement, High-resolution AFM imaging of single-stranded DNA-binding (SSB) protein--DNA complexes, Nucleic Acids Res. 35 (2007) e58–e58. https://doi.org/10.1093/nar/gkm147.

[36] M.E. Ferrari, W. Bujalowski, T.M. Lohman, Co-operative Binding of Escherichia coli SSB Tetramers to Single-stranded DNA in the (SSB)35

Binding Mode, J. Mol. Biol. 236 (1994) 106–123. https://doi.org/10.1006/jmbi.1994.1122.

[37] A.G. Kozlov, T.M. Lohman, Kinetic Mechanism of Direct Transfer of Escherichia coli SSB Tetramers between Single-Stranded DNA Molecules, Biochemistry. 41 (2002) 11611–11627. https://doi.org/10.1021/bi020361m.

[38] S.N. Savvides, S. Raghunathan, K. Fütterer, A.G. Kozlov, T.M. Lohman, G. Waksman, The C-terminal domain of full-length E. coli SSB is disordered even when bound to DNA., Protein Sci. 13 (2004) 1942–7. https://doi.org/10.1110/ps.04661904.

[39] P.R. Bianco, The tale of SSB, Prog. Biophys. Mol. Biol. 127 (2017) 111–118. https://doi.org/10.1016/j.pbiomolbio.2016.11.001.

[40] T. Paradžik, Ž. Filić, D. Vujaklija, Variations in amino acid composition in bacterial single stranded DNA–binding proteins correlate with GC content, Period. Biol. 118 (2017). https://doi.org/10.18054/pb.v118i4.4847.

[41] K. Dubiel, A.R. Myers, A.G. Kozlov, O. Yang, J. Zhang, T. Ha, T.M. Lohman, J.L. Keck, Structural Mechanisms of Cooperative DNA Binding by Bacterial Single-Stranded DNA-Binding Proteins, J. Mol. Biol. 431 (2019) 178–195. https://doi.org/10.1016/j.jmb.2018.11.019.

[42] G.M. Harami, Z.J. Kovács, R. Pancsa, J. Pálinkás, V. Baráth, K. Tárnok, A. Málnási-Csizmadia, M. Kovács, Phase separation by ssDNA binding protein controlled via protein−protein and protein−DNA interactions, Proc. Natl. Acad. Sci. 117 (2020) 26206–26217. https://doi.org/10.1073/pnas.2000761117.

[43] T. Zhao, Y. Liu, Z. Wang, R. He, J. Xiang Zhang, F. Xu, M. Lei, M.B. Deci, J.

Nguyen, P.R. Bianco, Super-resolution imaging reveals changes in Escherichia coli SSB localization in response to DNA damage, Genes to Cells. 24 (2019) 814–826. https://doi.org/10.1111/gtc.12729.

[44] P.R. Bianco, S. Pottinger, H.Y. Tan, T. Nguyenduc, K. Rex, U. Varshney, The IDL of E. coli SSB links ssDNA and protein binding by mediating protein-protein interactions, Protein Sci. 26 (2017) 227–241. https://doi.org/10.1002/pro.3072.

[45] N.J. Bonde, C. Henry, E.A. Wood, M.M. Cox, J.L. Keck, Interaction with the carboxy-terminal tip of SSB is critical for RecG function in E. coli, Nucleic Acids Res. 51 (2023) 3735–3753. https://doi.org/10.1093/nar/gkad162.

[46] U. Curth, J. Genschel, C. Urbanke, J. Greipel, In Vitro and in Vivo Function of the C-Terminus of Escherichia Coli Single-Stranded DNA Binding Protein, Nucleic Acids Res. 24 (1996) 2706–2711. https://doi.org/10.1093/nar/24.14.2706.

[47] C. Lindner, R. Nijland, M. van Hartskamp, S. Bron, L.W. Hamoen, O.P. Kuipers, Differential Expression of Two Paralogous Genes of Bacillus subtilis Encoding Single-Stranded DNA Binding Protein, J. Bacteriol. 186 (2004) 1097–1105. https://doi.org/10.1128/JB.186.4.1097-1105.2004.

[48] Y.-H. Huang, C.-Y. Huang, SAAV2152 is a single-stranded DNA binding protein: the third SSB in Staphylococcus aureus, Oncotarget. 9 (2018) 20239–20254. https://doi.org/10.18632/oncotarget.24427.

[49] T. Paradzik, N. Ivic, Z. Filic, B.A. Manjasetty, P. Herron, M. Luic, D. Vujaklija, Structure–function relationships of two paralogous single-stranded DNA-binding proteins from Streptomyces coelicolor: implication of SsbB in

chromosome segregation during sporulation, Nucleic Acids Res. 41 (2013) 3659–3672. https://doi.org/10.1093/nar/gkt050.

[50] A. Singh, U. Varshney, M. Vijayan, Structure of the second Single Stranded DNA Binding protein (SSBb) from Mycobacterium smegmatis, J. Struct. Biol. 196 (2016) 448–454. https://doi.org/10.1016/j.jsb.2016.09.012.

[51] D.E. Grove, S. Willcox, J.D. Griffith, F.R. Bryant, Differential Single-stranded DNA Binding Properties of the Paralogous SsbA and SsbB Proteins from Streptococcus pneumoniae, J. Biol. Chem. 280 (2005) 11067–11073. https://doi.org/10.1074/jbc.M414057200.

[52] D.E. Grove, F.R. Bryant, Effect of Mg2+ on the DNA Binding Modes of the Streptococcus pneumoniae SsbA and SsbB Proteins, J. Biol. Chem. 281 (2006) 2087–2094. https://doi.org/10.1074/jbc.M510884200.

[53] I. Mijakovic, Bacterial single-stranded DNA-binding proteins are phosphorylated on tyrosine, Nucleic Acids Res. 34 (2006) 1588–1596. https://doi.org/10.1093/nar/gkj514.

[54] J.G. Glanzer, J.L. Endres, B.M. Byrne, S. Liu, K.W. Bayles, G.G. Oakley, Identification of inhibitors for single-stranded DNA-binding proteins in eubacteria, J. Antimicrob. Chemother. 71 (2016) 3432–3440. https://doi.org/10.1093/jac/dkw340.

[55] T. Yadav, B. Carrasco, A.R. Myers, N.P. George, J.L. Keck, J.C. Alonso, Genetic recombination in Bacillus subtilis : a division of labor between two single-strand DNA-binding proteins, Nucleic Acids Res. 40 (2012) 5546–5559. https://doi.org/10.1093/nar/gks173.

[56] T. Yadav, B. Carrasco, E. Serrano, J.C. Alonso, Roles of Bacillus subtilis DprA and SsbA in RecA-mediated Genetic Recombination, J. Biol. Chem. 289 (2014) 27640–27652. https://doi.org/10.1074/jbc.M114.577924.

[57] L. Attaiech, A. Olivier, I. Mortier-Barrière, A.-L. Soulet, C. Granadel, B. Martin, P. Polard, J.-P. Claverys, Role of the Single-Stranded DNA–Binding Protein SsbB in Pneumococcal Transformation: Maintenance of a Reservoir for Genetic Plasticity, PLoS Genet. 7 (2011) e1002156. https://doi.org/10.1371/journal.pgen.1002156.

[58] Z. Stefanic, D. Vujaklija, L. Andrisic, G. Mikleusevic, M. Andrejasic, D. Turk, M. Luic, Preliminary Crystallographic Study of Streptomyces coelicolor Single-stranded DNA-binding Protein, Croat. Chem. Acta. 80 (2007) 35–39.

[59] Z. Štefanić, D. Vujaklija, M. Luić, Structure of the single-stranded DNA-binding protein from Streptomyces coelicolor, Acta Crystallogr. Sect. D Biol. Crystallogr. 65 (2009) 974–979. https://doi.org/10.1107/S0907444909023634.

[60] P. Radivojac, L.M. Iakoucheva, C.J. Oldfield, Z. Obradovic, V.N. Uversky, A.K. Dunker, Intrinsic Disorder and Functional Proteomics, Biophys. J. 92 (2007) 1439–1456. https://doi.org/10.1529/biophysj.106.094045.

[61] E.J. Choi, S.L. Mayo, Generation and analysis of proline mutants in protein G, Protein Eng. Des. Sel. 19 (2006) 285–289. https://doi.org/10.1093/protein/gzl007.

[62] M.W. MacArthur, J.M. Thornton, Influence of proline residues on protein conformation, J. Mol. Biol. 218 (1991) 397–412. https://doi.org/10.1016/0022-2836(91)90721-H.

[63] W. Ding, H.Y. Tan, J.X. Zhang, L.A. Wilczek, K.R. Hsieh, J.A. Mulkin, P.R. Bianco, The mechanism of <scp>Single strand binding protein–RecG</scp> binding: Implications for <scp>SSB</scp> interactome function, Protein Sci. 29 (2020) 1211–1227. https://doi.org/10.1002/pro.3855.

[64] X. Jin, J.-E. Lee, C. Schaefer, X. Luo, A.J.M. Wollman, A.L. Payne-Dwyer, T. Tian, X. Zhang, X. Chen, Y. Li, T.C.B. McLeish, M.C. Leake, F. Bai, Membraneless organelles formed by liquid-liquid phase separation increase bacterial fitness, Sci. Adv. 7 (2021). https://doi.org/10.1126/sciadv.abh2929.

[65] A.K. Lancaster, A. Nutter-Upham, S. Lindquist, O.D. King, PLAAC: a web and command-line application to identify proteins with prion-like amino acid composition, Bioinformatics. 30 (2014) 2501–2502. https://doi.org/10.1093/bioinformatics/btu310.

[66] B. Bolognesi, N. Lorenzo Gotor, R. Dhar, D. Cirillo, M. Baldrighi, G.G. Tartaglia, B. Lehner, A Concentration-Dependent Liquid Phase Separation Can Cause Toxicity upon Increased Protein Expression, Cell Rep. 16 (2016) 222–231. https://doi.org/10.1016/j.celrep.2016.05.076.

[67] R.M. Vernon, P.A. Chong, B. Tsang, T.H. Kim, A. Bah, P. Farber, H. Lin, J.D. Forman-Kay, Pi-Pi contacts are an overlooked protein feature relevant to phase separation, Elife. 7 (2018). https://doi.org/10.7554/eLife.31486.

[68] R.M. Vernon, J.D. Forman-Kay, First-generation predictors of biological protein phase separation, Curr. Opin. Struct. Biol. 58 (2019) 88–96. https://doi.org/10.1016/j.sbi.2019.05.016.

[69] X.-C. Su, Y. Wang, H. Yagi, D. Shishmarev, C.E. Mason, P.J. Smith, M. Vandevenne, N.E. Dixon, G. Otting, Bound or Free: Interaction of the C-

Terminal Domain of Escherichia coli Single-Stranded DNA-Binding Protein (SSB) with the Tetrameric Core of SSB, Biochemistry. 53 (2014) 1925–1934. https://doi.org/10.1021/bi5001867.

[70] K.R. Williams, E.K. Spice, M.B. LoPrestig, R.A. Guggenheimerl, J.W. Chase, Limited Proteolysis Studies on the Escherichia coli Single-stranded DNA Binding Protein, J. Biol. Chem. 258 (1983) 3346–3355.

[71] M. Green, L. Hatter, E. Brookes, P. Soultanas, D.J. Scott, Defining the Intrinsically Disordered C-Terminal Domain of SSB Reveals DNA-Mediated Compaction, J. Mol. Biol. 428 (2016) 357–364. https://doi.org/10.1016/j.jmb.2015.12.007.

[72] N. Golub, A. Meremyanin, K. Markossian, T. Eronina, N. Chebotareva, R. Asryants, V. Muronets, B. Kurganov, Evidence for the formation of start aggregates as an initial stage of protein aggregation, FEBS Lett. 581 (2007) 4223–4227. https://doi.org/10.1016/j.febslet.2007.07.066.

[73] C.E. Mason, S. Jergic, A.T.Y. Lo, Y. Wang, N.E. Dixon, J.L. Beck, Escherichia coli Single-Stranded DNA-Binding Protein: NanoESI-MS Studies of Salt-Modulated Subunit Exchange and DNA Binding Transactions, J. Am. Soc. Mass Spectrom. 24 (2013) 274–285. https://doi.org/10.1007/s13361-012-0552-2.

[74] M.K. Shinn, A.G. Kozlov, B. Nguyen, W.M. Bujalowski, T.M. Lohman, Are the intrinsically disordered linkers involved in SSB binding to accessory proteins?, Nucleic Acids Res. (2019). https://doi.org/10.1093/nar/gkz606.

[75] K. Saikrishnan, J. Jeyakanthan, J. Venkatesh, N. Acharya, K. Sekar, U. Varshney, M. Vijayan, Structure of Mycobacterium tuberculosis Single-

stranded DNA-binding Protein. Variability in Quaternary Structure and Its Implications, J. Mol. Biol. 331 (2003) 385–393. https://doi.org/10.1016/S0022-2836(03)00729-0.

[76] K. Saikrishnan, G.P. Manjunath, P. Singh, J. Jeyakanthan, Z. Dauter, K. Sekar, K. Muniyappa, M. Vijayan, Structure of Mycobacterium smegmatis single-stranded DNA-binding protein and a comparative study involving homologus SSBs: biological implications of structural plasticity and variability in quaternary association, Acta Crystallogr. Sect. D Biol. Crystallogr. 61 (2005) 1140–1148. https://doi.org/10.1107/S0907444905016896.

[77] P.S. Kaushal, P. Singh, A. Sharma, K. Muniyappa, M. Vijayan, X-ray and molecular-dynamics studies on Mycobacterium leprae single-stranded DNA-binding protein and comparison with other eubacterial SSB structures, Acta Crystallogr. Sect. D Biol. Crystallogr. 66 (2010) 1048–1058. https://doi.org/10.1107/S0907444910032208.

[78] B. Yu, B.M. Pettitt, J. Iwahara, Dynamics of Ionic Interactions at Protein–Nucleic Acid Interfaces, Acc. Chem. Res. 53 (2020) 1802–1810. https://doi.org/10.1021/acs.accounts.0c00212.

[79] L.T. Fernández-Martínez, M.J. Bibb, Use of the Meganuclease I-SceI of Saccharomycescerevisiae to select for gene deletions in actinomycetes, Sci. Rep. 4 (2014) 7100. https://doi.org/10.1038/srep07100.

[80] B. Gust, G. Chandra, D. Jakimowicz, T. Yuqing, C.J. Bruton, K.F. Chater, λ Red-Mediated Genetic Manipulation of Antibiotic-Producing Streptomyces, in: 2004: pp. 107–128. https://doi.org/10.1016/S0065-2164(04)54004-2.

[81] J. Schwedock, J.R. McCormick, E.R. Angert, J.R. Nodwell, R. Losick,

Assembly of the cell division protein FtsZ into ladder-like structures in the aerial hyphae of Streptomyces coelicolor, Mol. Microbiol. 25 (1997) 847–858. https://doi.org/10.1111/j.1365-2958.1997.mmi507.x.

[82] K. Katoh, J. Rozewicki, K.D. Yamada, MAFFT online service: multiple sequence alignment, interactive sequence choice and visualization, Brief. Bioinform. 20 (2019) 1160–1166. https://doi.org/10.1093/bib/bbx108.

[83] C.T. Rueden, J. Schindelin, M.C. Hiner, B.E. DeZonia, A.E. Walter, E.T. Arena, K.W. Eliceiri, ImageJ2: ImageJ for the next generation of scientific image data, BMC Bioinformatics. 18 (2017) 529. https://doi.org/10.1186/s12859-017-1934-z.